



Full Length Article

Role of CdSe quantum dots in the structure and antibacterial activity of chitosan/poly ϵ -caprolactone thin filmsM.S. Meikhail^a, A.M. Abdelghany^{b,*}, W.M. Awad^a^a Physics Department, Faculty of Science, Mansoura University, 35516 Mansoura, Egypt^b Spectroscopy Department, Physics Division, National Research Center, 33 ElBehouth St., 12311 Dokki, Giza, Egypt

ARTICLE INFO

Article history:

Received 4 January 2018

Received in revised form 18 April 2018

Accepted 2 May 2018

Available online 12 May 2018

Keywords:

CdSe

QDs

Ch/PCL

FTIR

SEM

Antibacterial tests

ABSTRACT

Chitosan/polycaprolactone (Ch/PCL) semi-natural polymeric blend containing gradient concentrations of CdSe quantum dots (QDs) dopant were synthesized via hot injection method. Synthesized samples containing different concentration of CdSe QDs were characterized by X-ray diffraction and FTIR absorption spectroscopy. FTIR experimental data of synthesized samples shows the maintenance of characteristic vibrational band with a marginal variation in both intensity and position related to the increase in dopant concentration. XRD patterns reveal amorphous nature of prepared virgin blend and blend samples that contain small amount of QDs. Samples with higher QDs concentration, namely (0.008, 0.016) wt% show appearance of crystalline bands related to the (1 1 1) reflection plane and in agreement with JCPDS card no. 19-0191. Scanning electron microscopy (SEM) indicates that morphology of synthesized biocomposites is critically affected by addition of CdSe QDs.

Antibacterial tests reveals different inhibition zone related to increasing concentration of CdSe QDs and type of bacteria under investigation. Evaluation of The activity index % were also studied.

© 2018 Mansoura University. Production and hosting by Elsevier B.V. This is an open access article under the CC BY-NC-ND license (<http://creativecommons.org/licenses/by-nc-nd/4.0/>).

1. Introduction

Chitosan is a natural polymer classified as polysaccharide that composed of a random distribution of β -(1-4)-linked D-glucosamine and N-acetyl-D-glucosamine with a chemical formula $(C_6H_{11}O_4N)_n$ [1] which can be obtained from deacetylation process of chitin that considered as the second most abundant polysaccharide primarily extracted from exoskeleton of sea creatures [2–4]. Chitosan gained its cationic nature due to amino groups that grants biological activity at low pH values that results in a high capacity to interact with negatively charged compounds including proteins or anionic polysaccharides.

Poly ϵ -caprolactone (PCL) is a hydrophobic synthetic semi-crystalline polyester with the chemical formula $(C_6H_{10}O_2)_n$ that synthesized by ring opening polymerization of monomer (ϵ -caprolactone) via cationic, anionic and co-ordination catalysts or by free radical ring-opening polymerization of 2-methylene-1-3-dioxepane [5]. PCL usually characterized by slow degradation rate combined with high plasticity and ductility that can help counter balance the rapid degradation of natural polymers and

increase the structural stability of the scaffolds obtained from their blends [6,7].

Blending of natural and synthetic polymers namely PCL with cellulose, starch and chitin may result in a new class of materials suitable with desired properties for bio-application as unique [8–12]. The hydrophobic character of PCL decreases the physico-chemical interactions with cells laying on its surface and their blends considered as a good candidate for the construction of 3D scaffolds results from slow degradation rate and its ability to maintain its morphology and mechanical properties after implanted that enhance mechanical properties of chitosan based scaffolds especially in the wet state [13]. PCL/Ch blends have been used as scaffold materials in the controlled release of drugs like Ofloxacin [14] and in nerve tissue reconstruction [15]. Ch/PCL ratio of 75/25 has higher hydrophilicity and better mechanical properties and cell adhesion and proliferation than PCL scaffolds.

Quantum dots (QDs) are spherical nano-sized crystals that may be formed of almost all semiconducting metals including CdSe, CdS, CdTe, PbS and ZnS while, alloys or any other metals may be used [16,17]. Cadmium selenide (CdSe) may be considered as an archetypal quantum dot with size range from 2 to 10 nm in diameter (10–50 atoms). Many types of quantum dot will emit light of specific frequencies if electricity or light is applied to them. These frequencies can be precisely tuned by changing the dot's size, [18,19], giving rise to many applications. QDs were introduced to

* Corresponding author.

E-mail address: a.m.abdelghany@yahoo.com (A.M. Abdelghany).

biological cell as alternative fluorescent probes in recent years. It uses in biological imaging, bio-sensing and intracellular detection and targeting, solar cells, quantum computing, transistors, LEDs and diode lasers [20]. Density function theory (DFT) is computational quantum mechanical method utilized as a part of physical science, material science to research the electronic structure (the ground state) of numerous body system, specifically particles, and atoms. It is a standout amongst the most well-known and effective quantum mechanical ways to deal with matter.

The present work aims to introduce a routine characterization for a novel semi-natural polymeric blend containing gradient concentration of CdSe QDs. FTIR, density functional theory (DFT) and XRD was employed to approve the reaction mechanisms between both constituents of organic matrix and that with inorganic dopant. In addition, the antimicrobial tests were performed to study the effect of CdSe QDs on different gram-positive, gram-negative and fungi.

2. Experiment and method

2.1. Materials

Chitosan of molecular weight 6.0×10^5 [2-Amino-2-deoxy-(1-4)glucopyranan] with the chemical formula $(C_8H_{11}NO)_n$, supplied by Aldrich Co. Poly ϵ -caprolactone of average molecular weight 45,000 with chemical formula $(C_6H_{10}O_2)_n$, supplied by Aldrich in pellets form. Acetic acid, ethanol and other solvents of high purity were supplied by Sham Lab. Co.

2.2. Sample preparation

CdSe QDs were synthesized via ordinary hot injection route previously reported [21,22]. In the synthesis route 0.8 mmol of CdO was added to about 20 mmol of stearic acid in a tri-neck flask with smooth heating (70–110 °C) in nitrogen atmosphere. The temperature was raised gradually to 180 °C after the formation of cadmium stearate (colorless solution). One mmol of Se metal powder and 3 mL of trioctylphosphine (TOP) were injected to the flask. Six equal amount of reaction mixture were collected every 15 min to permit the QDs formation and growth. The samples were instantaneously cooled and diluted with toluene to discontinue CdSe particles growth. Obtained QDs were washed in methanol media and centrifuged.

Chitosan and poly ϵ -caprolactone were dissolved in 0.2 M aqueous acetic acid and glacial acetic acid respectively. Ch/ PCL (75/25) poly blend was prepared using casting technique. Gradient concentration of the QDs were added to form thin film of desired concentrations. Samples were kept in evacuated dissector until use. Table 1 lists the abbreviation and sample composition.

2.3. Physical measurements

Single beam (Nicolet iS10, USA) spectrophotometer was used to record the FTIR experiment data in the spectral range (4000–400)

cm^{-1} and with resolution of $2\ cm^{-1}$ to study the vibrational mode of the specimens.

X-ray diffraction scans were obtained using PANalytical X'Pert PRO XRD system using Cu K_{α} target with secondary monochromator (where, $\lambda = 1.540\ \text{\AA}$, the tube operated at 45 kV–40 mA (Holland), the Bragg's angle (2θ) in the range of (5–80°). In this analysis, the peak locations (2θ) in X-ray diffraction spectra are used to identify the different crystalline structures in the pure and doped films.

The morphology of the films was characterized by scanning electron microscope using SEM Model Quanta 250 FEG (Field Emission Gun) with accelerating voltage 30 kV, magnification $14\times$ up to 1,000,000 and resolution for Gun.1n). Size and shape of QDs determined using HRTEM (JEOL-JEM-2100) with accelerating voltage 200 kV while UV/Vis. measurement was performed using JASCO V770 Spectrophotometer.

3. Results and discussions

3.1. Characterization of prepared QDs

Fig. 1 reveals UV UV/Vis optical absorption spectra of prepared CdSe QDs combined with high resolution transmission electron micrographs (HRTEM). Obtained micrograph shows that synthesized material are of spherical shape with size ranging from 4 to 5 nm. UV/Vis. optical absorption spectrum was found to be in agreement with that reported for the same sample previously reported [21,22].

3.2. Fourier transform-infrared spectroscopy (FTIR)

FTIR absorption experimental data of prepared pristine polymeric matrices and their blend films shown in Fig. 2 reveals the maintenance of basic vibrational groups belong to the backbone matrices of both Ch and PCL. The absorption bands observed in the chitosan spectra at $2951, 2872\ cm^{-1}$ can be assigned to the stretching vibrations of CH_3 , while bands at $1648, 1555\ cm^{-1}$ may be attributed to $(-C=O)$ secondary amide and $(-C=O)$ protonated amine stretching respectively. Other bands located at $1165, 1025\ cm^{-1}$ are assigned to $(C-O-C)$ a symmetric and $(C-O-C)$ symmetric vibration respectively. The band at $3429, 1724, 1412\ cm^{-1}$ is assigned to $(O-H)$ overlapped to the $(N-H)$ stretching vibrations, $(C=O)$ carbonyl stretching and (CH_3) symmetric deformation. Same observation with marginal variation in peak position and/or intensity may be observed for PCL films. Fig. 3 also, shows

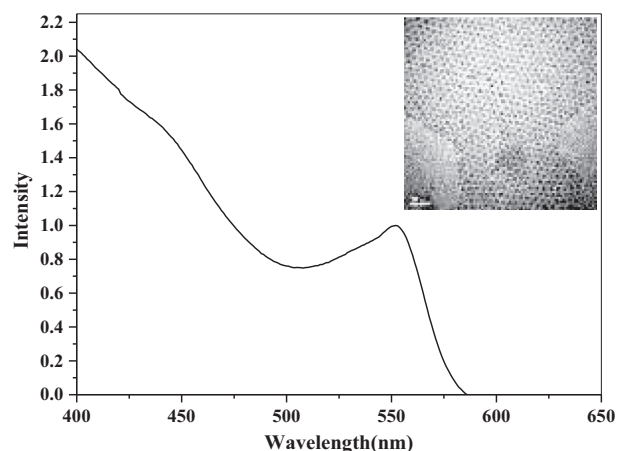


Fig. 1. Reveals UV UV/Vis optical absorption spectra of prepared CdSe QDs combined with high resolution transmission electron micrographs.

Table 1
Sample notation and composition.

Sample	Chitosan wt%	PCL	CdSe
CdSe0	75	25	0.000
CdSe1	75	25	0.001
CdSe2	75	25	0.002
CdSe4	75	25	0.004
CdSe8	75	25	0.008
CdSe16	75	25	0.016

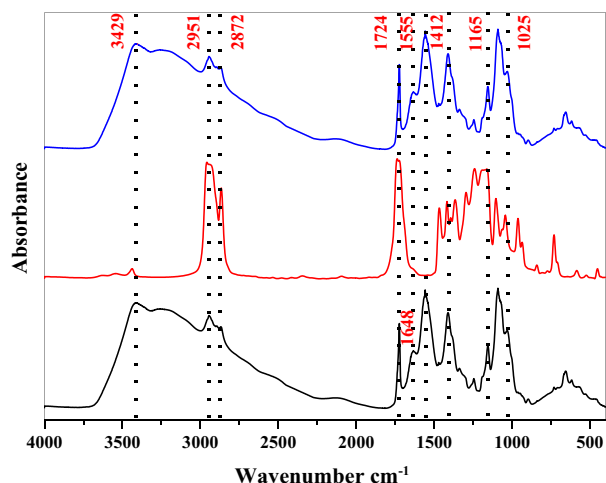


Fig. 2. FTIR absorption spectra of chitosan and PCL blend.

distinct changes in the blend spectrum indicating some type of interaction between individual blend constituents. Such interaction can be discussed using both experimental and theoretical approach discussed in the next sections. Fig. 3 shows FTIR spectra of prepared polymeric blend doped with different concentrations of the inorganic filler (CdSe QDs). Analysed data of synthesized samples can be shown in Table 2. An obvious change in intensity was observed with increasing CdSe dopant content. The peaks at 1025 and 1412 cm^{-1} appear sharp in blend and (CdSe1) then become broad and increase in the broadness with increase concentration of filler up to 0.008 wt% then disappear in concentration of 0.016. The intensity of the peaks at 1555 cm^{-1} and 1724 cm^{-1} decrease with increasing filler until concentration 0.016 cm^{-1} , peak is disappeared. FTIR spectra are used to investigate the incorporation of PCL into chitosan biopolymer matrices by showing the absorption band positions and the vibrational modes.

3.3. Density function theory (DFT)

Density Functional Theory (DFT) a theoretical approach is employed to identify mechanism of interaction between the polymer matrices and measure the degree of agreement with

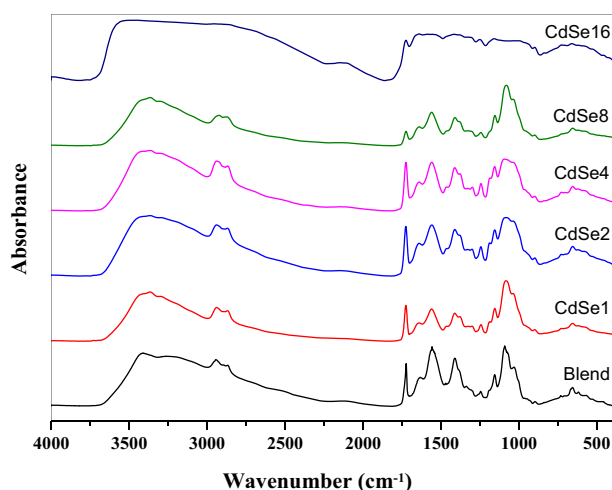


Fig. 3. FTIR absorption spectra of chitosan and PCL blend with different concentration of CdSe QDs.

Table 2

FTIR spectral data of prepared polymeric matrices and their assignments [23–25].

Peak position (cm^{-1})	Band assignment	References
3429	(O—H) overlapped to the (N—H) stretching vibrations	23
2951	(CH ₂) asymmetric stretching	23
2872	(CH ₂) symmetric stretching	24
1724	(C=O) carbonyl stretching	24
1648	(C=O) stretching	23
1555	(C=O) stretching protonated amine	25
1412	(CH ₃) symmetric deformation	25
1165	(C—O—C) symmetric stretching	24
1025	(C—O—C) a symmetric and (C—O—C) symmetric vibration	25

experimental data for complex interaction between both chitosan and Poly ϵ -caprolactone.

All calculations were performed using Gaussian 03 programs [26] within the DFT framework. Polymeric blend of (Ch/PCL) was optimized using the Becke's three parameter hybrid functional, (B3LYP) correlation functional was also employed with the electron core potential basis set WLANL2DZ [27,28].

Both experimental and theoretical FTIR spectrum of Ch/PCL binary blend and polymer blend with dopant QDs are perceived to be in agreement with the suggested interaction and complexation between samples constituents shown in both Fig. 4a:d.

3.4. X-ray diffraction analysis

The X-ray diffraction analysis for both pure chitosan and pure PCL show a broad band corresponding to amorphous nature of chitosan and two characteristic peaks at angles $2\theta = 21.2^\circ$ and $2\theta = 23.5^\circ$, corresponding to the (1 1 0) and (2 0 0) crystallographic planes of semi crystalline nature of PCL biopolymer as shown in Fig. 5. XRD patterns of the Chitosan/PCL blend show that the two characteristic peaks of PCL were disappeared indicates the miscibility among two biopolymers, which means that the incorporation of PCL did not significantly affect the amorphous structure of chitosan. From Fig. 6, we can observed that the XRD patterns of the Ch/PCL/CdSe QDs bio-composites still kept the amorphous structure of Ch/PCL blend until the concentration of (0.008, 0.016) wt% of CdSe nanoparticles, two characteristic peaks of CdSe appear in concentration (0.008) wt% and make overlapping to form one peak in concentration (0.016) wt% which means that CdSe nanoparticles affect significantly on the amorphous structure of the blend.

3.5. Scanning electron microscope (SEM)

The SEM has been used to explore the surface morphology and structure of studied samples, Fig. 7(A, B) presents SEM the micrographs of pure chitosan and pure PCL which showed smooth appearance of the surface. The SEM of Ch/PCL blend as shown in Fig. 7(C), doesn't show any new features.

Addition of CdSe, QDs, with different concentrations to the biopolymer blend, the surface of bio composites become rough and the grain size was formed and varied in their shape according to CdSe QDs concentration as shown in Fig. 6(D–H). It is clear that the grain size at high concentration (0.008, 0.016) of CdSe QDs takes a definite shape and the CdSe were dispersed well in the blend. That's mean that the morphology of Ch/PCL/CdSe QDs bio-composites is critically affected by addition of CdSe QDs. This reveals compatibility between the SEM and X-ray response of the present Ch/PCL/CdSe system.

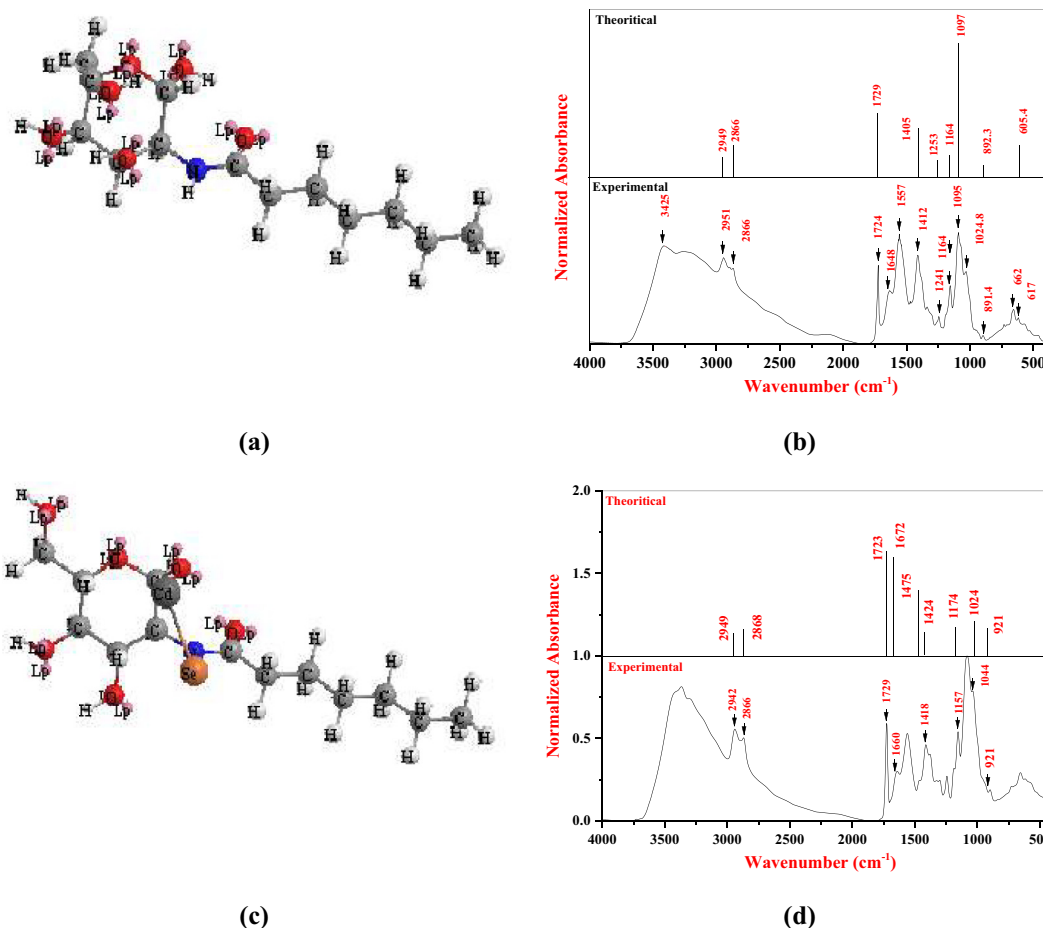


Fig. 4. (a) Schematic diagram of optimized suggested interaction mechanism between Ch and PCL. (b) Theoretical and experimental FTIR data of prepared polymer blend. (c) Schematic diagram of optimized suggested interaction mechanism of polymer blend and CdSe QDs. (d) Theoretical and experimental FTIR data of prepared composite.

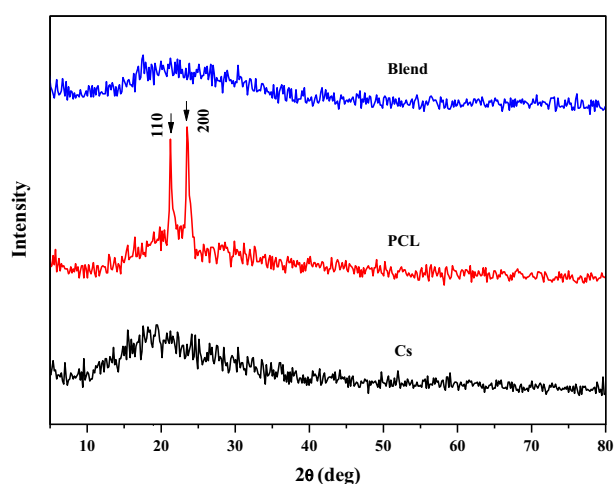


Fig. 5. X-ray diffraction of pure chitosan, pure PCL and chitosan/PCL blend.

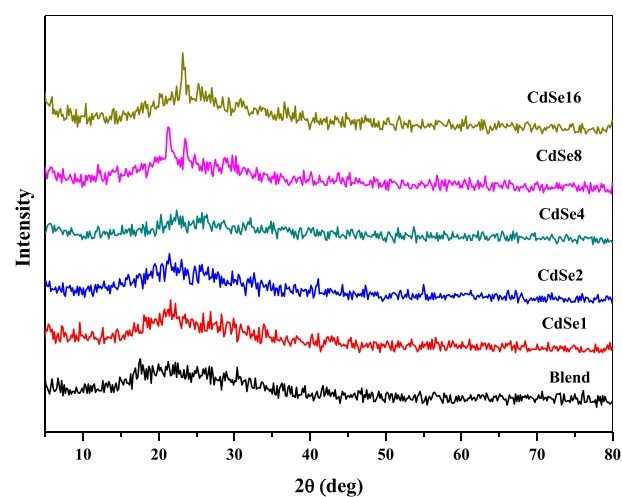


Fig. 6. X-ray diffraction of Ch/PCL/CdSe QDs biocomposites.

3.6. Antibacterial tests

During the last decade significant interest has aroused in the research on synthesis of Cadmium selenide (CdSe) QDs for biological, biomedical and pharmaceutical applications due to their known antimicrobial properties. The Cadmium ion exhibits broad-spectrum biocidal activity towards many different bacteria, fungi, and viruses [29–31].

The antimicrobial activity of the synthesized CdSe QDs doped with different concentration in polymer blend were tested. Thus the antimicrobial activity of the compounds was evaluated against two gram-positive (*Staphylococcus aureus*, *Bacillus subtilis*) and two gram-negative bacteria (*Pseudomonas aeruginosa* and *Escherichia coli*) as well as against the pathogenic fungus *Candida albicans* (*C. albicans*). The samples were seeded in petri dishes containing agar

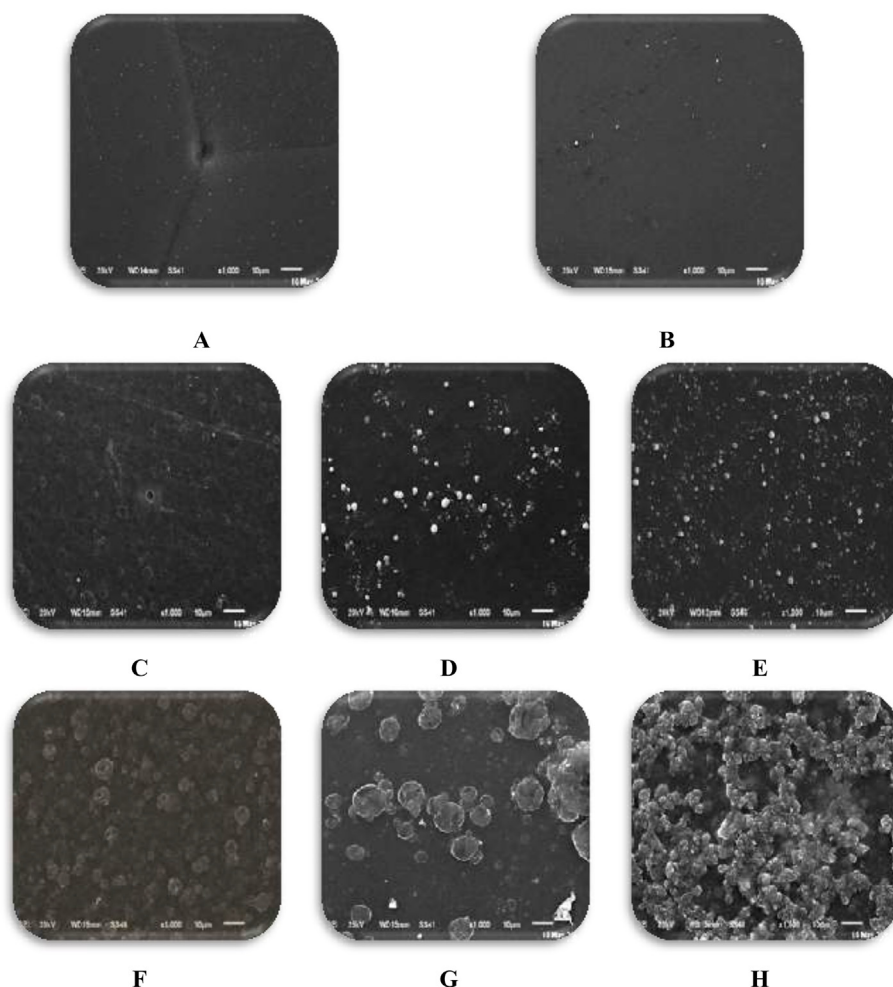


Fig. 7. A (Chitosan), B (PCL), C (Blend), D (CdSe1), E (CdSe2), F (CdSe4), G (CdSe8), H (CdSe16).

media (Agar 20 g + Beef extract 3 g + peptone 5 g) and the petri dishes were incubated at 36 °C. The inhibition zones were recorded after 24 h of incubation and summarized in Table 3. Each treatment was replicated three times.

Thus the antimicrobial activity percent (%) was evaluated from the relation:

$$\% \text{Activity Index} = \frac{\text{Zone of inhibition by test compound (diameter)}}{\text{Zone of inhibition by standard (diameter)}} \times 100$$

Fig. 8 shows antibacterial test results of CdSe QDs doped in polymer blend at room temperatures (RT). It was found that the size of the inhibition zone was higher against *Bacillus subtilis* and *Staphylococcus aureus* at 0.001 wt% CdSe QDs. Antibacterial activities index were found against all test cultures (*Staphylococcus aureus*, *Bacillus subtilis*) to be 83.3 and 52.2 respectively. While the activity index for *Escherichia coli* and *Pseudomonas aeruginosa* were 50.0 and 82.6 respectively. Moreover, the activity index of *Candida Fungi* was 81.5 at concentration 0.002 wt% CdSe QDs.

Table 3
concentration of CdSe QDs against the diameter of inhibition zone and the activity index %.

No.	Compound	<i>E. coli</i> (mg/ml)		<i>Pseudomonas aeruginosa</i> (mg/ml)		<i>S. aureus</i> (mg/ml)		<i>Bacillus subtilis</i> (mg/ml)		<i>C. albicans</i> (mg/ml)	
		D (mm)	A %	D (mm)	A %	D (mm)	A %	D (mm)	A %	D (mm)	A %
1	Chitosan	17.0	65.4	21	91.3	22.0	91.7	13.0	56.5	18.0	66.7
2	Blend	NA	–	5	21.7	7.00	29.2	4.00	17.4	2.00	7.40
3	CdSe(1)	13.0	50.0	19	82.6	20.0	83.3	12.0	52.2	4.00	14.8
4	CdSe(2)	9.00	34.6	13	56.5	9.0	37.5	7.0	30.4	22.0	81.5
5	CdSe(4)	12.0	46.1	17	73.9	19.0	79.2	10.0	43.5	15.0	55.5
6	CdSe(8)	NA	–	NA	–	5.00	20.8	NA	–	5.00	18.5
7	CdSe(16)	7.00	26.9	9	39.1	12.0	50.0	8.00	34.8	3.00	11.1
	Ampicillin	26.0	100	23.0	100	24.0	100	23.0	–	NA	–
	Clotrimazole	NA	–	NA	–	NA	–	NA	–	27	100

D, Diameter of inhibition zone; A, Activity index and NA no observed action.




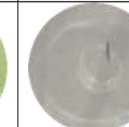
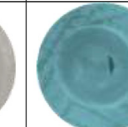



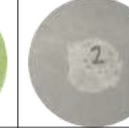


























Sample	<i>C. Albicans</i> (mg/ml) (Fungi)	<i>Bacillus subtilis</i> (mg/ml) (gram positive)	<i>S. aureus</i> (mg/ml) (gram positive)	<i>Pseudomonas</i> <i>aeruginosa</i> (mg/ml) (gram-negative)	<i>E. coli</i> (mg/ml) (gram-negative)
Chitosan					
Blend					
CdSe1					
CdSe2					
CdSe4					
CdSe8					
CdSe16					

Fig. 8. The inhibition zone vs. the concentration of CdSe QDs.

No antibacterial activity was found at 0.008 wt% CdSe QDs except for *Staphylococcus aureus* and *Candida albicans* they show a moderate index activity and small inhibition zone. Among all, *Bacillus subtilis* exhibited maximum susceptibility, while *Pseudomonas aeruginosa* was found to be least susceptible to CdSe QDs. Increasing the synthesizing concentration of CdSe QDs resulted in significant reduction of antibacterial activity of CdSe may be due to increase in particle size of CdSe QDs. The difference of the sizes of zone of inhibition between the CdSe QDs synthesized at different concentration could be correlated to the difference in nanoparticles diffusion tendency in cells due to the difference in their sizes producing different amount of reactive oxygen species (ROS).

The size of inhibition zone was different according to the type of bacteria and the concentrations of CdSe QDs. Based on the results obtained from Fig. 8 and the diameter of inhibition zone for different bacteria, it can be concluded that the maximum inhibition activity happens for *Staphylococcus aureus*. Fig. 8 also, demonstrates the similar extended results for different concentrations of CdSe nanoparticles antibacterial activity and it can be seen that the same results obtained. The maximum diameter has happened for *S. aureus*. All numerical data can be tabulated as seen in Table 3.

4. Conclusion

Semi-natural biocomposite of Ch/PCL containing gradient concentrations of CdSe QDs were successfully synthesized and

characterized through X-ray diffraction and FTIR absorption spectroscopy. DFT approach was employed to investigate the reaction mechanisms of both polymer blend and samples that doped with the QDs filling material. Both FTIR experimental and experimental data shows the maintenance of characteristic vibrational band with a marginal variation in both intensity and position related to the increase in dopant concentration. XRD patterns reveal amorphous nature of prepared virgin blend and blend samples that contain small amount of QDs. Samples with higher QDs concentration, namely CdSe8 and CdSe16 shows appearance of crystalline bands assigned to 111 reflection plane reported previously and in agreement with JCPDS card no. 19-0191. Scanning electron microscopy (SEM) indicates that morphology of synthesized bio-composites is critically affected by addition of CdSe QDs. Antibacterial tests reveals different inhibition zone related to increasing concentration of CdSe QDs and sort of bacterial strain under investigation. Evaluation of The activity index % were also studied.

References

- [1] Dash M, Chiellini F, Ottenbrite RM, Chiellini E. Chitosan-A versatile semi-synthetic polymer in biomedical applications. *Prog Polym Sci* 2011;36 (8):981–1014.
- [2] Monier M, Abdel-Latif DA, Abou El-Reash YG. Ion-imprinted modified chitosan resin for selective removal of Pd(II) ions. *J Colloid Interface Sci* 2016;469:344–54.

- [3] Liu J, Meng Cg, Liu S, Kan J, Jin Ch. Preparation and characterization of protocatechuic acid grafted chitosan films with antioxidant activity. *Food Hydrocolloids* 2017;63:457–66.
- [4] Lin YC, Wang HP, Gohar F, Ullah MH, Zhang X, Xie DF, et al. Preparation and copper ions adsorption properties of thiosemicarbazide chitosan from squid pens. *Int J Biol Macromol* 2017;95:476–83.
- [5] Pitt CG. Poly-ε-caprolactone and its copolymers. In: Chasin M, Langer R, editors. *Biodegradable polymers as drug delivery systems*. New York: Marcel Dekker; 1990. p. 71–120.
- [6] Labet M, Thielemans W. Synthesis of polycaprolactone: a review. *Chem Soc Rev* 2009;38:3484–504.
- [7] Li WJ, Cooper JA, Mauck RL, Tuan RS. Fabrication and characterization of six electrospun poly(hydroxy ester)-based fibrous scaffolds for tissue engineering applications. *Acta Biomater* 2006;2:377–85.
- [8] Yang K, Wang XL, Wang YZ. Progress in nanocomposite of biodegradable polymer. *J Ind Eng Chem* 2007;13(4):485–500.
- [9] Hong S, Kim GH. Fabrication of electrospun polycaprolactone biocomposites reinforced with chitosan for the proliferation of mesenchymal stem cells. *Carbohydr Polym* 2011;83:940–6.
- [10] Ghorbani FM, Kaffashi B, Shokrollahi P. PCL/chitosan/Zn-doped nHA electrospun nanocomposite scaffold promotes adipose derived stem cells adhesion and proliferation. *Carbohydr Polym* 2015;118:133–42.
- [11] Sahoo S, Sasmal A, Sahoo D. Synthesis and characterization of chitosan–polycaprolactone blended with organoclay for control release of doxycycline. *J Appl Polym Sci* 2010;118:3167–75.
- [12] Abdolmohammadi S, Siyamak S, Ibrahim NA. Enhancement of mechanical and thermal properties of polycaprolactone/chitosan blend by calcium carbonate nano-particles. *Int J Mol Sci* 2012;13:4508–22.
- [13] Raftery RM. Development of a gene-activated scaffold platform for tissue engineering applications using chitosan–pDNA nanoparticles on collagen-based scaffolds. *J Controlled Release* 2015;210:84–94.
- [14] Sahoo S, Sasmal A, Nanda R. Synthesis of chitosan polycaprolactone blend for control delivery of ofloxacin drug. *Carbohydr Polym* 2010;79:106–13.
- [15] Bolaina-Lorenzo E, Martínez-Ramos C, Monleón-Pradas M, Herrera-Kao W, Cauch-Rodríguez JV, Cervantes-Uc JM. Electrospun polycaprolactone/chitosan scaffolds for nerve tissue engineering: physicochemical characterization and Schwann cell biocompatibility. *Biomed Mater* 2016;12(1):01500.
- [16] Bailey RE, Nie S. Alloyed semiconductor quantum dots, tuning the optical properties without changing the particle. *J Am Chem Soc* 2003;125:7100–6.
- [17] Sabaeian M, Nasab AK. Size-dependent intersubband optical properties of dome-shaped InAs/GaAs quantum dots with wetting layer. *Appl Opt* 2012;51(18):4176–85.
- [18] Nasab AK, Sabaeian M, Sahrai M, Fallahi Kerr V. Nonlinearity due to intersubband transitions in a three-level InAs/GaAs quantum dot, the impact of a wetting layer on dispersion curves. *J Opt* 2014;16(5):055004.
- [19] Ramírez H, Flórez YJ, Camacho AS. Efficient control of coulomb enhanced second harmonic generation from excitonic transitions in quantum dot ensembles. *J Phys Chem Chem Phys* 2015;17(37).
- [20] Bruchez M, Moronne M, Gin P, Weiss S, Alivisatos AP. Semiconductor nanocrystals as fluorescent biological labels. *Science* 1998;281(5385):2013–6.
- [21] Tananaev PN, Dorofeev SG, Vasil'ev RB, Kuznetsova TA. Preparation of copper-doped CdSe nanocrystals. *Inorg Mater* 2009;45:347–51.
- [22] Hu MZ, Zhu T. Semiconductor nanocrystal quantum dot synthesis approaches towards large-scale industrial production for energy applications. *Nanoscale Res Lett* 2015;10(1):469–83.
- [23] Gautam S, Chou C, Dinda AK, Potdar PD, Mishra NC. Fabrication and characterization of PCL/gelatin/chitosan ternary nanofibrous composite scaffold for tissue engineering applications. *J Mater Sci* 2014;49:1076–89.
- [24] Elzubair A, Elias CN, Suarez JCM, Lopes HP, Vieira MVB. The physical characterization of a thermoplastic polymer for endodontic obturation. *J Dent* 2006;34:784–9.
- [25] Silva SML, Braga CRC, Fook MVL, Raposo CMO, Carvalho LH, Canedo EL. Application of infrared spectroscopy to analysis of chitosan/clay nanocomposites. *Mater Sci Eng Technol* 2012. ISBN 978-953-51-0537-4.
- [26] Frisch MJ, Trucks GW, Schlegel HB, Scuseria GE, Robb MA, et al. *Gaussian 03, Revision A.1*. Pittsburgh PA: Gaussian Inc; 2003.
- [27] Hay PJ, Wadt WR. Ab initio effective core potentials for molecular calculations. Potentials for the transition metal atoms Sc to Hg. *J Chem Phys* 1985;82:270.
- [28] Becke D. Density-functional thermochemistry. III. The role of exact exchange. *J Chem Phys* 1993;98:5648.
- [29] Kloepfer JA, Mielke RE, Nadeau JL. *Appl Environ Microb* 2005;71:2548.
- [30] Wang L, Zheng H, Long Y, Gao M, Hao J, Du J, et al. *Hazard J Mater* 2010;177:1134.
- [31] Kim YG, Moon S, Kuritzkes DR, Demirci U. *Biosens Bioelectron* 2009;25:253.